

Focusing of atoms with strongly confined light potentials

Lars Egil Helseth

*Department of Physics, University of Oslo,
P.O. Box 1048 Blindern, N-0316 Oslo, Norway*

Abstract

Focusing of atoms with light potentials is studied. In particular, we consider strongly confined, cylindrical symmetric potential, and demonstrate their applications in both red and blue-detuned focusing of atoms. We also study the influence of aberrations, and find that a resolution of 1 nm should in principle be possible.

arXiv:quant-ph/0205184v2 3 Nov 2002

I. INTRODUCTION

Focusing of light is of importance both in fundamental studies and for technical applications. Microscopy, spectroscopy, optical data storage are only a few of the fields utilizing focused light. The first treatments of electromagnetic focusing problems are due to Ignatowsky[1]. However, the detailed structure of the wave-field in the focal region was clarified by Wolf and coworkers, who did the first detailed studies of electromagnetic focusing systems[2, 3, 4]. Here the so-called Debye approximation was adopted, where only the plane waves with propagation vectors that fall inside the geometrical cone whose apex is at the focal point contribute to the field in the focal region[2, 5]. The Debye approximation predicts that the electromagnetic field is symmetrical about the focal plane. However, later it was found that the Debye theory is valid only when the focal point is located many wavelengths away from the aperture, and the angular aperture is sufficiently large[6]. When these conditions are not fulfilled, the electromagnetic field is not symmetrical about the focal plane[7, 8, 9, 10].

Recently, focusing of spatially inhomogeneous polarization distributions have triggered a lot of interest due to their potential applications in data storage and for manipulation of molecules[11, 12, 13, 14]. Such distributions may be efficiently produced by spatial light modulators (e.g. LCD's) or interferometric methods[15, 16, 17, 18]. The potential of these polarization distributions is not yet fully exploited, and many interesting discoveries may occur in the future. Of particular interest here is effective focusing of atoms.

Focusing of neutral atoms using light has attracted considerable interest the last 25 years, since the atomic wavelength is much smaller than the optical wavelength, and because atoms interact with matter in a different manner than other particles. An atom in a radiation field experiences two different forces[19, 20]. The spontaneous emission force results from absorption and random spontaneous emission of photons, and is basically radiation pressure. The magnitude of this force is limited by the rate of spontaneous emission, and saturates as the laser intensity increases. The second force is the so-called gradient or dipole force, which derives from the interaction of the induced atomic dipole moment with the nonuniform light distribution. It can be made arbitrary large by increasing the intensity gradient, and is dependent on the amount of detuning from the atomic resonance frequency. For red-detuned light the force is in the direction of increasing intensity, whereas for blue-detuned light the

sign of the force is reversed. The first demonstration of focusing of an atomic beam with the dipole force was presented by Bjorkholm et al. [21, 22]. They showed that using a red-detuned continuous wave laser a spot size of $28 \mu m$ is obtainable. The resolution was here limited by spontaneous emission processes, which effectively introduced aberrations in the focused beam. Later Balykin et al. reported experiments using two counterpropagating laser beams acting as an atom lens[23, 24]. In this way they were able to demonstrate imaging of atomic sources, but were limited by similar aberrations as Bjorkholm et al.[21, 22]. To avoid this, Balykin and Letokhov suggested the application of a hollow, blue-detuned laser beam. This dipole potential has the advantage that the atoms go through a region of low intensity, so that the spontaneous emission is rather small. Two more detailed studies of this type of lens were later presented in Refs. [25, 26].

More recently, focusing of atoms using a standing wave field has attracted considerable attention[27, 28, 29, 30, 31, 32, 33, 34, 35]. When an atomic beam is incident transverse to a standing wave field, the field gradient acts as a sequence of lenses for the atoms. At the focal plane the atomic spatial distribution consists of a periodic set of lines or dots distanced from each other by $\lambda/2$, where λ is the wavelength of the light. Atomic beams of Na, metastable He and Cr has been focused using standing wave fields[27, 33, 34, 35]. With Cr widths as small as a few tens of nanometers have been produced[30]. However, it has been pointed out that its application in atomic lithography is restricted, since arbitrary patterns cannot be produced. Thus, some alternative methods have been suggested. For example, it has been proposed that it is possible to form an atom lens using the near field from a fiber tip, thus obtaining resolutions of less than 10 nm[36]. A particularly interesting proposal was given by Dubetsky and Berman[37]. They proposed to use a conical mirror and an inhomogeneously polarized pulsed laser beam to obtain the wanted dipole potential. This configuration is in many ways similar to that of Bjorkholm et al., but avoids the problems with spontaneous emission aberrations.

In the current paper we investigate how a strongly confined light potential can be used to focus atoms. We are particularly interested in beams with cylindrical symmetry, since these provide a symmetric optical potential. To that end, we first need to determine the properties of such light potentials. Here we use the Debye approximation to calculate the electric field in the focal region. In particular, it is found that a radially polarized beam may be used in red-detuned focusing, whereas the azimuthal distribution is useful for blue-detuned focusing.

II. HIGH APERTURE FOCUSING OF LIGHT

In previous studies only weakly focused light was considered[23, 25]. However, it is also of interest to consider strongly confined light potentials generated by high aperture focusing. Such potentials may give higher intensity gradients and shorter atomic focal lengths, which is of interest in certain applications. However, if linearly polarized light is strongly focused, the light intensity is no longer symmetric in the focal region, which may reduce the resolution of an atom focusing system. Thus, it is necessary to examine the properties of strongly focused light more carefully. We start by assuming that our focusing system has high angular aperture and that the focal point is placed many wavelengths away from the aperture. Then the diffracted field near the focal plane can be calculated in the Debye approximation as[7]

$$\mathbf{E} = -\frac{ikC}{2\pi} \int \int_{\Omega} \mathbf{T}(\mathbf{s}) \exp[ik(s_x x + s_y y + s_z z)] ds_x ds_y , \quad (1)$$

where C is a real constant, $k = 2\pi/\lambda$ is the wavenumber, $\mathbf{s} = (s_x, s_y, s_z)$ is the unit vector along a typical ray, Ω is the solid angle formed by all the geometrical rays, $\mathbf{T}(\mathbf{s})$ is the vector pupil distribution which accounts for the polarization, phase and amplitude distributions at the exit pupil.

In spherical coordinates, the unit wave vector is defined as

$$\mathbf{s} = (\sin\theta \cos\phi, \sin\theta \sin\phi, \cos\theta) . \quad (2)$$

The position vector can be written as

$$\mathbf{r}_c = (r_c \sin\theta_c \cos\phi_c, r_c \sin\theta_c \sin\phi_c, z) . \quad (3)$$

This gives the following diffraction integral:

$$\mathbf{E} = -\frac{iC}{\lambda} \int_0^\alpha \int_0^{2\pi} \mathbf{T}(\theta, \phi) \exp[ik\kappa] \sin\theta d\theta d\phi , \quad (4)$$

where α is the convergence semiangle and

$$\kappa = z \cos\theta + r_c \sin\theta \sin\theta_c \cos(\phi - \phi_c) . \quad (5)$$

The amplitude vector for each ray is given by

$$\mathbf{T}(\theta, \phi) = \mathbf{P}(\theta, \phi) B(\theta, \phi) , \quad (6)$$

where $\mathbf{P}(\theta, \phi)$ is the polarization distribution and $B(\theta, \phi)$ the amplitude and phase distribution at the exit pupil. We emphasize that $B(\theta, \phi)$ can be used to describe any focusing systems (with lenses and mirrors). For an aplanatic system $B(\theta) = \sqrt{\cos\theta}$. Other examples are found in Ref. [7].

The state of the polarization incident on the focusing system influences the structure of the electric field near the focal plane. To discuss this question quantitatively, we must find a general expression for the polarization vector. To this end, we assume a polarization which may in general depend on the polar and azimuthal angles

$$\mathbf{P}_0 = \begin{bmatrix} a(\theta, \phi) \\ b(\theta, \phi) \\ 0 \end{bmatrix} .$$

Then the polarization vector can be written as

$$\mathbf{P}(\theta, \phi) = R^{-1}CRP_0 . \quad (7)$$

Here \mathbf{R} describes the rotation of the coordinate system around the optical axis

$$\mathbf{R} = \begin{bmatrix} \cos\phi & \sin\phi & 0 \\ -\sin\phi & \cos\phi & 0 \\ 0 & 0 & 1 \end{bmatrix} ,$$

and \mathbf{C} describes the change of polarization on propagation through the lens

$$\mathbf{C} = \begin{bmatrix} \cos\theta & 0 & \sin\theta \\ 0 & 1 & 0 \\ -\sin\theta & 0 & \cos\theta \end{bmatrix} .$$

The result is

$$\mathbf{P}(\theta, \phi) = \begin{bmatrix} a[\cos\theta\cos^2\phi + \sin^2\phi] + b[\cos\theta\sin\phi\cos\phi - \sin\phi\cos\phi] \\ a[\cos\theta\cos\phi\sin\phi - \sin\phi\cos\phi] + b[\cos\theta\sin^2\phi + \cos^2\phi] \\ -a\sin\theta\cos\phi - b\sin\theta\sin\phi \end{bmatrix} .$$

The procedure presented above can be used to calculate the electric field in the focal region for any combinations of polarization, phase and amplitude distributions at the exit pupil. Here we will consider only two different polarization distributions; radial and azimuthal

polarized light, see Fig. 1. In both cases a singularity occurs at the origin. Thus, practical generation of these beams usually involves blocking out the central portion of the beam. However, in our theoretical calculations the singularity does not affect the results, and we may ignore it (but keeping in mind its existence).

A. Radial polarization

In the case of radial polarization we may write $a(\phi) = \cos\phi$ and $b(\phi) = \sin\phi$, which results in the following expression:

$$\mathbf{P}(\theta, \phi) = \begin{bmatrix} \cos\theta\cos\phi \\ \cos\theta\sin\phi \\ -\sin\theta \end{bmatrix} .$$

When inserted in Eq. (4), this gives

$$E_x^{rad} = \frac{2C\pi}{\lambda} I_1^{rad} \cos\phi_c , \quad (8)$$

$$E_y^{rad} = \frac{2C\pi}{\lambda} I_1^{rad} \sin\phi_c , \quad (9)$$

$$E_z^{rad} = -\frac{2C\pi i}{\lambda} I_0^{rad} , \quad (10)$$

where

$$I_0^{rad} = \int_0^\alpha B(\theta) \sin^2\theta J_0(kr_c \sin\theta \sin\theta_c) \exp(ikz\cos\theta) d\theta , \quad (11)$$

and

$$I_1^{rad} = \int_0^\alpha B(\theta) \cos\theta \sin\theta J_1(kr_c \sin\theta \sin\theta_c) \exp(ikz\cos\theta) d\theta . \quad (12)$$

Here the z component is completely independent of the azimuthal angle, and its importance increases with increasing angular aperture. In Fig. 2 $|E_z|^2$ (solid line) and $|E_x|^2$ (dash-dotted line) are shown for the case $B(\theta) = \sqrt{\cos\theta}$, $\alpha = 80^\circ$ and $\phi_c = 0^\circ$. Here the peak of $|E_x|^2$ is only 5 % of $|E_z|^2$. The x component can be made much smaller by using an aperture which blocks out the central part of the beam. The dashed line in Fig. 2 shows the case when $\alpha_1 = 70^\circ$ has been blocked out and the total semiconvergence angle is $\alpha = 80^\circ$. Note that although the central lobe has shrunk, more energy is distributed into the sidelobes.

This is a general feature valid not only for radially polarized light (see e.g. Ref. [7] and references therein).

Let us now consider an annular aperture with $\alpha \sim 90^\circ$, $B=1$ and where most of the central part (except the rim) of the exit pupil is blocked out. Then the x and y components of the electric field at the focal plane are almost zero. On the other hand, for $z=0$ the z component can be approximated by

$$E_z^{rad} \approx -\frac{2C_1\pi i}{\lambda} J_0(kr_c) , \quad (13)$$

where C_1 is a constant. We assume here that all the light is distributed into the transmitting zone in order to optimize the light intensity. This can be done by using a holographic beamshaper or an axicon combined with a proper lens system[38]. Close to the geometric focal point the intensity becomes

$$I^r = \frac{1}{2\eta} |E_z^{rad}|^2 \approx \frac{2}{\eta} \left(\frac{C_1\pi}{\lambda} \right)^2 \left(1 - \frac{(kr_c)^2}{2} \right) , \quad (14)$$

where $\eta = 377 \Omega$ is the impedance of vacuum. We see that near the maximum the intensity behaves as a parabola, which may be useful for focusing of atoms.

B. Azimuthal polarization

Another polarization mode of interest is the azimuthal distribution. In this case we may write $a = \sin\phi$ and $b = -\cos\phi$, which results in

$$\mathbf{P}(\theta, \phi) = \begin{bmatrix} \sin\phi \\ -\cos\phi \\ 0 \end{bmatrix} .$$

When inserted in Eq. (4), we find:

$$E_x^{asi} = \frac{2C\pi}{\lambda} I_1^{asi} \sin\phi_c , \quad (15)$$

$$E_y^{asi} = -\frac{2C\pi}{\lambda} I_1^{asi} \cos\phi_c , \quad (16)$$

$$E_z^{asi} = 0 , \quad (17)$$

where

$$I_1^{asi} = \int_0^\alpha B(\theta) \sin\theta J_1(kr_c \sin\theta \sin\theta_c) \exp(ikz \cos\theta) d\theta . \quad (18)$$

As expected, the electric field near focus has no longitudinal component. Furthermore, we note that electric field vector is circularly symmetric, and is zero on the optical axis. In Fig. 3 the solid line shows the intensity $|E|^2$ at the focal plane for the case $B(\theta) = \sqrt{\cos\theta}$ and $\alpha = 30^\circ$. Note that the two peaks are located approximately λ away from the origin, and this distance is tuned by altering the angular aperture.

Let us now assume an annular aperture where $B=1$, $\alpha \sim 90^\circ$ and most of the exit pupil (except the rim) is blocked out. Then we may write (for $z=0$)

$$I^a \approx \frac{2\pi^2 C_1^2}{\lambda^2 \eta} J_1(kr_c) . \quad (19)$$

For small distances from the geometric focal point, the intensity can be written as

$$I^a \approx \frac{1}{2} \left(\frac{C_1 k \pi r_c}{\lambda} \right)^2 . \quad (20)$$

As for the radial polarization, the intensity near the focal point behaves as a parabola, but now the origin is at the minimum intensity.

III. ATOM FOCUSING

To calculate the the evolution of the atomic beam we use the path-integral technique of Refs. [25, 39]. Here the wave function is given by

$$\Psi(\mathbf{r}_b, t_b) = \int d^3\mathbf{r}_a K(\mathbf{r}_b, t_b, \mathbf{r}_a, t_a) \Psi(\mathbf{r}_a, t_a) , \quad (21)$$

where $\Psi(\mathbf{r}_a, t_a)$ is the initial wavefunction and $K(\mathbf{r}_b, t_b, \mathbf{r}_a, t_a)$ is the propagator

$$K(\mathbf{r}_b, t_b, \mathbf{r}_a, t_a) = \int_a^b \delta\mathbf{r} \exp \left[\left\{ \frac{i}{\hbar} S[\mathbf{r}(t)] \right\} \right] . \quad (22)$$

The integration is over all possible paths $\mathbf{r}(t)$ that starts at (\mathbf{r}_a, t_a) and ends at (\mathbf{r}_b, t_b) , and S denotes the action evaluated along that path:

$$S[\mathbf{r}(t)] = \int_{t_a}^{t_b} dt \left\{ \frac{m}{2} [\partial_t \mathbf{r}(t)]^2 - U(\mathbf{r}) \right\} . \quad (23)$$

In general, the spatial variations of the optical potential are slow compared to the atomic wavelength, which means that the propagator integral can be evaluated by the method of stationary phase, thus resulting in[25, 39]

$$K(\mathbf{r}_b, t_b, \mathbf{r}_a, t_a) \approx N \exp \left\{ \frac{i}{\hbar} S_c[\mathbf{r}(t)] \right\} . \quad (24)$$

This approximation is a semiclassical one, since $S_c[\mathbf{r}(t)]$ is now evaluated along the classical trajectory. N is in general a time and space dependent normalization factor which varies slowly compared with the phase factor, and is therefore neglected here. We now consider a collimated monoenergetic atomic beam travelling parallel to the optical axis with velocity \mathbf{V}_1 . Well defined collimation of Cr was demonstrated by Scholten *et al.*[40], and is therefore within the reach of current technology. The initial wave function can then be taken as

$$\Psi(\mathbf{r}_a, t_a) = \exp[ikz_a - (i/\hbar)Et_a] . \quad (25)$$

Ovchinnikov has pointed out the importance of using pulsed lasers for focusing of atoms in order to minimize spontaneous decay aberrations[41]. We will therefore assume that the potential is switched on and off so fast that the atomic kinetic energy does not change during the switching time, i.e. $\tau \ll 1/\omega$, where $\omega = \hbar k^2/2m$ is the recoil frequency of an atom with mass m . At the time $t = -\tau/2$ an optical pulse of duration τ is applied, thus resulting in an attraction or repulsion of the atoms. In fact, the intensity gradient of the laser beam results in a force $\mathbf{F} = -\nabla U(\mathbf{r})$, where

$$U(\mathbf{r}) = \frac{\hbar \Gamma^2 I}{8\Delta I_s} . \quad (26)$$

Here I is the laser intensity, I_s is the atomic transition saturation intensity, Γ is the natural linewidth, and $\Delta = \omega_L - \omega_R$ is the detuning of the laser frequency ω_L from the atomic resonance frequency ω_R . For this potential to be valid the laser must be detuned far from the transition, $|\Delta| \gg \Gamma$.

After the optical potential is turned off, the atoms again behave as free particles travelling with constant velocity, see Fig. 4. In fact, their wavefunctions represent a spherical wavefront converging to the focal region, where the aberrations depend on the detailed shape of the optical potential. The atoms move with a velocity given by

$$\mathbf{V}_2 = \frac{\mathbf{r}_a + \mathbf{R}}{t} . \quad (27)$$

Here $\mathbf{r}_a=(x_a, y_a, z_a)$ is the position vector from the aperture to the 'focal point', $\mathbf{R}=(x, y, z)$ is the position vector from the origin to the observation point, and t the time of flight. For a perfect optical potential, the focal distance is given by $f = V_2 t$.

We can write the classical action as

$$S_c[\mathbf{r}(t)] = \frac{m(\mathbf{r}_a + \mathbf{R})^2}{2t} - U(\mathbf{r})\tau . \quad (28)$$

Since we work with small angular apertures and assumes that $R \ll r_a$, the time of flight is nearly equal for all atoms, i.e. independent of position. Moreover, $V_2 \approx V_1$. If we consider only those atoms located near the focus of the optical potential, we can omit the integration over z_a , and the wavefunction in the focal region becomes

$$\Psi(x, y) \propto \int \int dx_a dy_a \exp \left[\frac{m\mathbf{r}_a \cdot \mathbf{R}}{\hbar t} + i\Phi(r_a) \right] , \quad (29)$$

where

$$\Phi(r_a) = \frac{m(x_a^2 + y_a^2)}{2\hbar t} - \frac{U(\mathbf{r}_a)\tau}{\hbar} . \quad (30)$$

Here the integration is taken over the aperture set up by the laser pulse. We see that the if the optical potential is harmonic, the quadratic phase-factor vanishes. This equation is similar to that of the electric field amplitude obtained in the scalar Debye approximation. Thus we may say that Eq. (29) is the Debye approximation for focusing of atoms.

Let us consider a circular aperture for the atomic beam. Then we may switch to cylindrical coordinates, and set

$$\mathbf{r}_a = (\rho \cos \gamma, \rho \sin \gamma, f - \frac{\rho^2}{2f}) , \quad (31)$$

and

$$\mathbf{R} = (r \cos \beta, r \sin \beta, z) , \quad (32)$$

where we have used the expansion $z_a = \sqrt{f^2 - \rho^2} \approx f - \frac{\rho^2}{2f}$, which is valid for reasonably small angular apertures. The wavefunction in the focal region is then expressed by

$$\Psi(r) \propto \int_0^a J_0 \left(\frac{2\pi \rho r}{\lambda_D f} \right) \exp \left(-i \frac{\pi \rho^2}{\lambda_D f^2} z \right) \exp [i\Phi(\rho)] \rho d\rho . \quad (33)$$

where a is the aperture radius and

$$\Phi(\rho) = \frac{\pi \rho^2}{\lambda_D f} - \frac{U(\rho)\tau}{\hbar} \quad (34)$$

To derive the wavefunction for this particular symmetry we have used the following identity:

$$\int_0^{2\pi} \exp(ik\rho\cos\phi)d\phi = 2\pi J_0(k\rho) . \quad (35)$$

Equation (33) is similar to that given in Ref.[42], but with the atomic de Broglie wavelength and a different aberration function. The atomic density can now be found by computing $|\Psi(r)|^2$. Although the similarities between focusing of light and atoms are well known[21, 24], we have not seen Eq. (33) been derived from a path-integral approach in any previous papers. Note in particular that Eq. (33) can be used to compute the wavefunction slightly away from focus for any potential of optic or magnetic origin, although this property will not be used here. On the other hand, it is also important to point out that this approximation is not valid for large convergence angles or large wavefront aberrations, as is also the case for the scalar Debye approximation for focusing of light[42] (Eq. (4) is the electromagnetic Debye approximation, which is valid for large convergence angles). Furthermore, the path-integral approach clearly does not take into account any polarization effects associated with e.g. permanently induced dipoles. That is, we assume that the only effect of the focused light is to give the atoms a 'kick' in the right direction. Finally, we have ignored the small effects which may be induced by the quantized electromagnetic field[43].

A. Red-detuned focusing

A red-detuned gradient potential utilizes a large and negative atom-field detuning, which means that the atom will be attracted to the high intensity region. To obtain a symmetrical wavefunction in the focal region, it is of importance that the gradient potential also is symmetric. To that end, both linear and radial polarization distributions may be used, but with certain restrictions. For example, focusing of linearly polarized light gives rise to both y and z components of the focused light which are proportional to $\sin 2\phi_c$ and $\cos\phi_c$, respectively. The z component may have a peak intensity of 25 % compared to the x component, and could therefore alter the gradient potential[11]. However, these effects are rather small as long as the angular aperture is kept sufficiently small. Here we will examine more closely focusing of atoms with a tightly focused radial laser beam. The advantage of such a scheme is that the beam is symmetric, and only the z component is significant when the angular aperture is large and the center beam is blocked out.

The radial polarization distribution is perhaps better suited to provide the necessary symmetry. In fact, we have seen that by using a large aperture combined with a suitable aperture, only the z component will be of importance. To that end, the aberration function is given by

$$\Phi(\rho) = \frac{\pi\rho^2}{\lambda_D f} - AJ_0^2(k\rho) , \quad (36)$$

where A is the so-called field area,

$$A = \frac{\tau k^2 C_1^2 \Gamma^2}{16\eta I_s \Delta} . \quad (37)$$

The field area is easily modulated by changing the power of the laser beam. Here we are mostly interested in a general description and will not be concerned with the exact laser power, which should be optimized in the particular experimental setup.

For small values of ρ , the focal distance in the laboratory frame is

$$f^r = \frac{\lambda^2}{2\pi A \lambda_D} . \quad (38)$$

In Fig. 5 f^r is plotted as a function of the field area for two different atoms with the same initial velocity (100 m/s). The solid line corresponds to ^{52}Cr with $m = 8.68 \times 10^{-26}$ kg and $\lambda = 0.43 \mu\text{m}$, whereas the dashed line corresponds to ^{23}Na with $m = 3.84 \times 10^{-26}$ kg and $\lambda = 0.59 \mu\text{m}$. One sees that typical focal distances range from a few microns to hundred microns. However, care must be taken when selecting the field area, since this together with the aperture determine the aberrations of the focusing system. Figure 6 shows the phase function (dash-dotted line) for Cr atoms with velocity 500 m/s and $A=-1$. It is seen that the phase function is nearly constant within an aperture of $\sim 0.1\mu\text{m}$, where the aberrations are negligible. Figure 7 shows $|\Psi(r)|^2$ for focusing of ^{52}Cr with a velocity of 500 m/s and aperture $a = 0.1 \mu\text{m}$. The solid line shows the atomic density when $A = -100$ (A is negative because the laser light is red-detuned), whereas the dashed line corresponds to $A=-20$. Here the focal lengths are 19 and 96 μm , respectively. We used a rather narrow atomic beam in order to block out most of the aberrations, thus allowing a resolution of ~ 1 nm ($A=-100$).

B. Blue-detuned focusing

In the case of blue-detuned focusing, the atom-field detuning is large and positive, $\Delta \gg \Gamma$. Thus, the atom will be expelled from the high intensity region. For this purpose the intensity

near the focal region of an azimuthal polarization distribution aberration may be useful. In this case the aberration function is

$$\Phi(\rho) = \frac{\pi\rho^2}{\lambda_D f} - AJ_1^2(k\rho) , \quad (39)$$

which is identical to that used by Dubetsky and Berman[37], except for the constant A. This is due to the fact that we consider here only the intensity gradient and neglect any effects of the polarization gradient. For small values of ρ , the focal distance in the laboratory frame is

$$f^a = \frac{\lambda^2}{\pi A \lambda_D} . \quad (40)$$

IV. DISCUSSION

Two systems for practical atom lithography are shown in Figs. 8 and 9, respectively. The first, which applies a 1D standing light wave, has been successfully adopted for focusing of many different atoms[44]. The disadvantage of this system is the low power and gradients (since the light is distributed over a large area). A more promising scheme for depositing atoms directly onto a transparent substrate is shown in Fig. 9. Here the atoms are incident on the opposite side of the substrate, and the lens system do not disturb the atomic beam. In practice the light beam should be slightly defocused on the far side of the substrate (where the atoms come in). Thus, if the light beam is properly corrected for the spherical aberrations introduced by the substrate, the electric field is the same as in Sec. II. We have shown that such a system could in principle give a resolution of 1 nm, but the system requirements are rather strict. Thus, it is indeed necessary to perform further investigations before a scheme similar to that of Fig. 9 can be applied in practice.

It has already been mentioned that the spontaneous emission aberrations must be reduced to a minimum in order to achieve a diffraction limited distribution. This can be obtained by using a pulsed laser beam, typically of pulse length 10 ns or shorter. Moreover, it is also of importance to reduce the chromatic aberrations. Again, a pulsed laser seems to be the solution, since then the focusing properties are less dependent on the atomic velocity. On the other hand, it should be pointed out that for an atom laser (where the atoms are monochromatic) chromatic aberrations are not a problem.

Notice that both for radial and azimuthal beams it is possible to alter the intensity

gradients by manipulating the phase and amplitude distribution at the exit pupil. A more general formulation of the electromagnetic field in presence of arbitrary exit pupils are found in Ref. [11]. By inserting an appropriate aperture it should be possible to manipulate the optical intensity gradient so that it looks more like a parabola. A further improvement would be to use an annular atomic beam. In this way one may use a smaller part of the optical potential. Then one may expect smaller aberration, since it should in principle be easier to make a small part of the optical intensity distribution look like a parabola than the whole atomic aperture. Naturally, this approach would lead to lower atomic densities, which in many applications is a big disadvantage.

V. CONCLUSION

Focusing of inhomogenously polarized light is studied, and expressions for the electric field in the focal region are given. It is seen that some polarization distributions at the exit pupil may give intensity distributions near the focal plane which are of interest for focusing of atoms. To this end, focusing of an atomic beam using near-resonant laser light is also studied, and the wave function in the focal region is found. Moreover, it is suggested how different light forces may be used in red and blue-detuned focusing of atoms.

-
- [1] V.S. Ignatowsky *Trans. Opt. Inst Petrograd I* , paper IV (1919).
 - [2] E. Wolf *Proc. Roy. Soc. A (London)* **253** , 349 (1959).
 - [3] B. Richards and E. Wolf *Proc. Roy. Soc. A (London)* **253** , 358 (1959).
 - [4] A. Boivin and E. Wolf *Phys. Rev.* **138** , B1561 (1965).
 - [5] P. Debye *Ann. Phys.* **30** , 755 (1909).
 - [6] E. Wolf and Y. Li *Opt. Commun.* **39** , 205 (1981).
 - [7] J.J. Stamnes *Waves in focal regions* Adam Hilger, Bristol, 1986.
 - [8] J.J. Stamnes and B. Spjelkavik *Opt. Commun.* **40** , 81 (1981).
 - [9] Y. Li and E. Wolf *Opt. Commun.* **39** , 211 (1981).
 - [10] V. Dhayalan and J.J. Stamnes *J. Pure Appl. Opt.* **6** , 347 (1997).
 - [11] L.E. Helseth *Opt. Commun.* **191**, 161 (2001).

- [12] K.S. Youngworth and T.G. Brown *Optics Express* **7** , 77 (2000).
- [13] D.P. Biss and T.G. Brown *Optics Express* **9** , 490 (2001).
- [14] L. Novotny, M.R. Beversluis, K.S. Youngworth and T.G. Brown *Phys. Rev. Lett.* **86** , 5251 (2001).
- [15] S.C. Tidwell, G.H. Kim and W.D. Kimura *Appl. Opt.* **32**, 5222 (1993).
- [16] S.C. Tidwell, D.H. Ford and W.D. Kimura *Appl. Opt.* **29**, 2234 (1990).
- [17] T. Grosjean, D. Corjoun and M. Spajer *Opt. Commun.* **203** , 1 (2002).
- [18] Z. Bomzon, G. Biener, V. Kleiner and E. Hasman *Opt. Lett.* **27**, 285 (2002).
- [19] A. Ashkin *Phys. Rev. Lett.* **40** , 729 (1978).
- [20] V.G. Minogin and V.S. Letokhov *Laser light pressure on atoms* Gordon and Breach Science Publishers, New York, 1987.
- [21] J.E. Bjorkholm, R.R. Freeman, A. Ashkin and D.B. Pearson *Phys. Rev. Lett.* **41** , 1361 (1978).
- [22] J.E. Bjorkholm, R.R. Freeman, A. Ashkin and D.B. Pearson *Opt. Lett.* **5** , 111 (1980).
- [23] V.I. Balykin, V.S. Letokhov, Y.B. Ovchinnikov and A.I. Sidorov *J. Mod. Opt.* **35** , 17 (1988).
- [24] V.I. Balykin and V.S. Letokhov *Opt. Commun.* **64** , 151 (1987).
- [25] G.M. Gallatin and P.L. Gould *J. Opt. Soc. Am. B* **8** , 502 (1991).
- [26] J.J. McClelland and M.R. Scheinfein *J. Opt. Soc. Am. B* **8** , 1974 (1991).
- [27] J.J. McClelland, R.E. Scholten, E.C. Palm and R.J. Celotta *Science* **262** , 877 (1993).
- [28] V. Natarajan, R.E. Behringer and G. Timp *Phys. Rev. A* **53** , 4381 (1996).
- [29] S. Meneghini, V.I. Savichev, K.A.H. van Leeuwen and W.P. Schleich *Appl. Phys. B* **70** , 675 (2000).
- [30] W.R. Anderson, C.C. Bradley, J.J. McClelland and R.J. Celotta *Phys. Rev. A* **59** , 2476 (1998).
- [31] J.L. Cohen, B. Dubetsky and P.R. Berman *Phys. Rev. A* **60** , 4886 (1999).
- [32] C.J. Lee *Phys. Rev. A* **61** , 063604 (2000).
- [33] M. Prentiss, G. Timp, N. Bigelow, R.E. Behringer and J.E. Cunningham *Appl. Phys. Lett.* **60** , 1027 (1992).
- [34] T. Sleator, T. Pfau, V. Balykin and J. Mlynek *Appl. Phys. B* **54** , 375 (1992).
- [35] G. Timp, R.E. Behringer, J.E. Cunningham, M. Prentiss and K. Berggren *Phys. Rev. Lett.* **69** , 1636 (1992).
- [36] V.I. Balykin, V.V. Klimov and V.S. Letokhov *J. Phys. II* **4** , 1981 (1994).

- [37] B. Dubetsky and P.R. Berman *Phys. Rev. A* **58** , 2413 (1998).
- [38] H.S. Lee, B.W. Stewart, K. Choi and H. Fenichel *Phys. Rev. A* **49** , 4922 (1994).
- [39] R.P. Feynman and A.R. Hibbs *Quantum Mechanics and Path Integrals* McGraw-Hill, New York, 1965.
- [40] R.E. Scholten, R. Gupta, J.J. McClelland, R.J. Celotta, M.S. Levenson and M.G. Vangel *Phys. Rev. A* **55** , 1331 (1996).
- [41] Y.B. Ovchinnikov *Opt. Commun.* **173** , 275 (2000).
- [42] M. Born and E. Wolf *Principles of Optics* 6th edition, p. 437, Cambridge University Press, UK, 1980.
- [43] B. Rohwedder and M. Orszag *Phys. Rev. A* **54** , 5076 (1996).
- [44] S.J. Rehse, R.W. McGowan and S.A. Lee *Appl. Phys. B* **70** , 657 (2000).

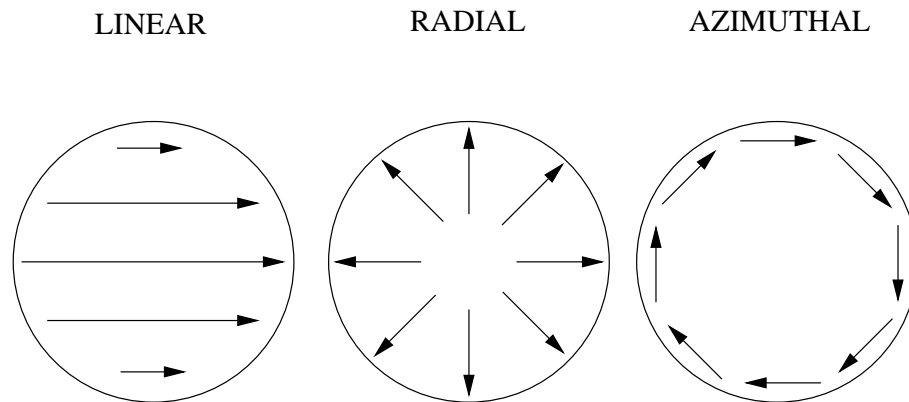


FIG. 1: The three different polarization modes considered in this paper.

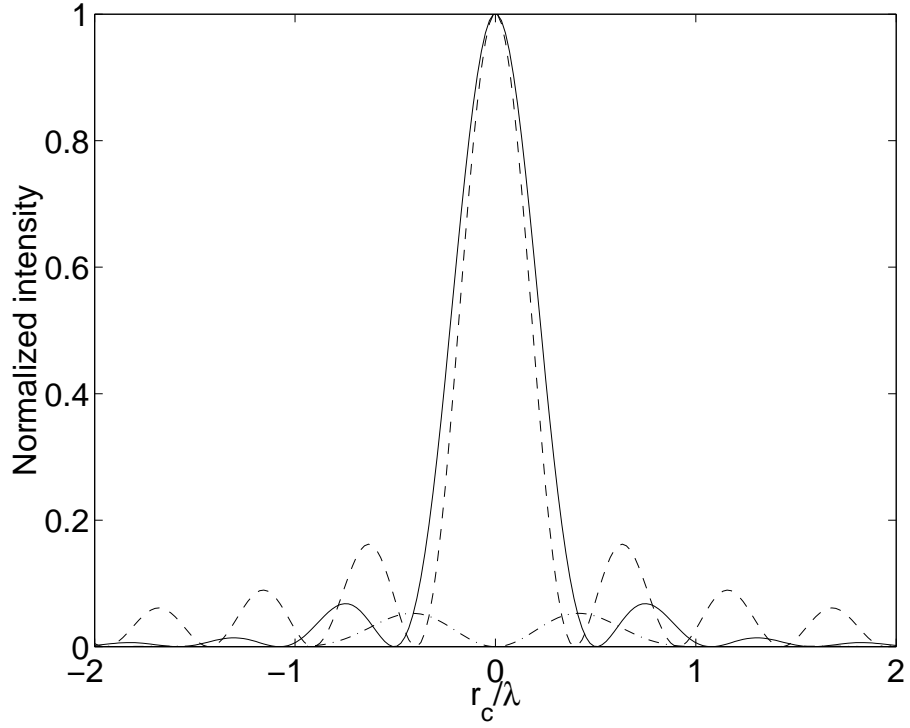


FIG. 2: $|E_z|^2$ (solid line) and $|E_x|^2$ (dash-dotted line) at the geometric focal point when $\alpha = 80^\circ$ and $\phi_c = 0^\circ$. The dashed line shows the case when only a narrow annular aperture is used (see text).

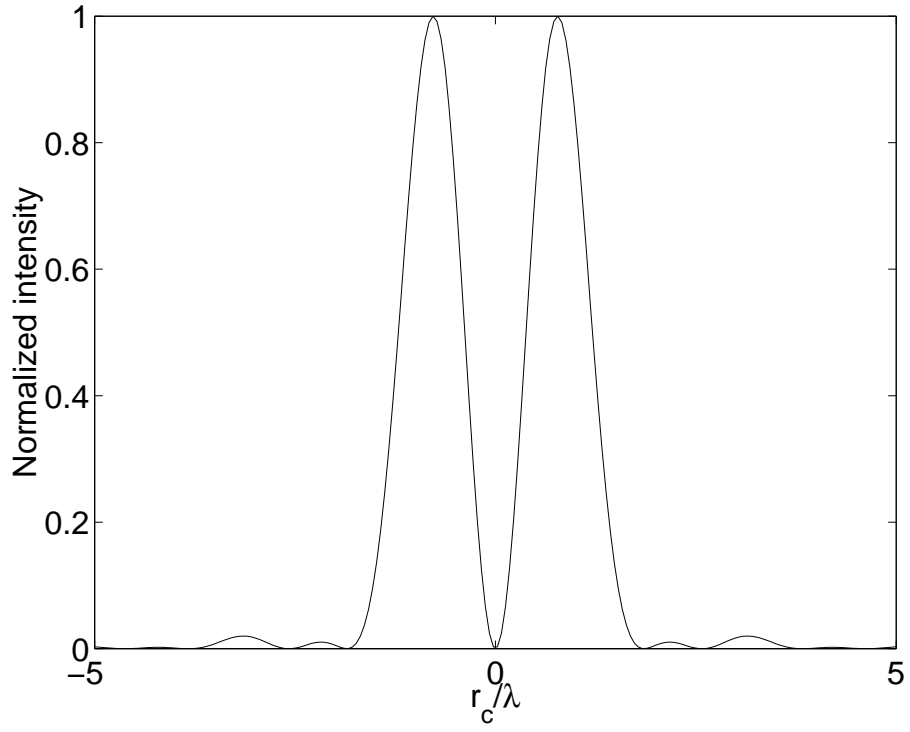


FIG. 3: $|E|^2$ at the focal point when $\alpha = 30^\circ$.

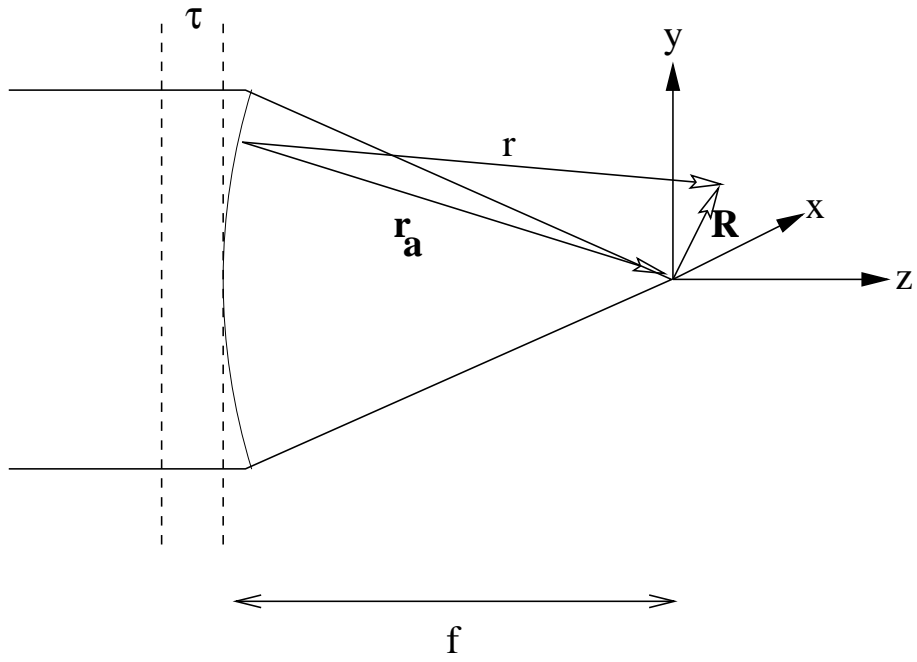


FIG. 4: Focusing of a collimated atomic beam.

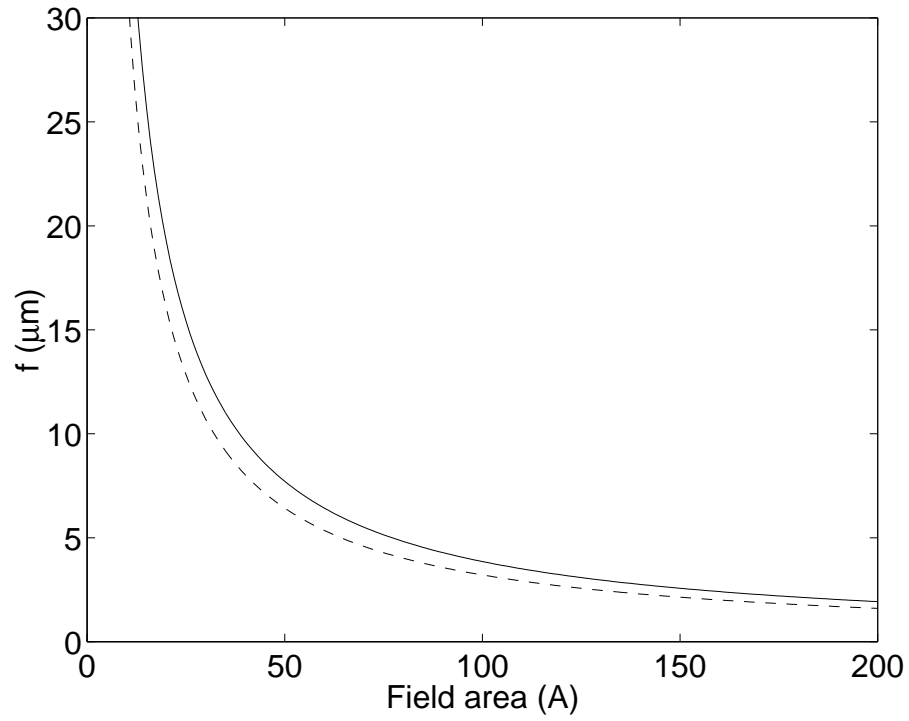


FIG. 5: The focal distance for focusing of ^{52}Cr (solid line) and ^{23}Na (dashed line).

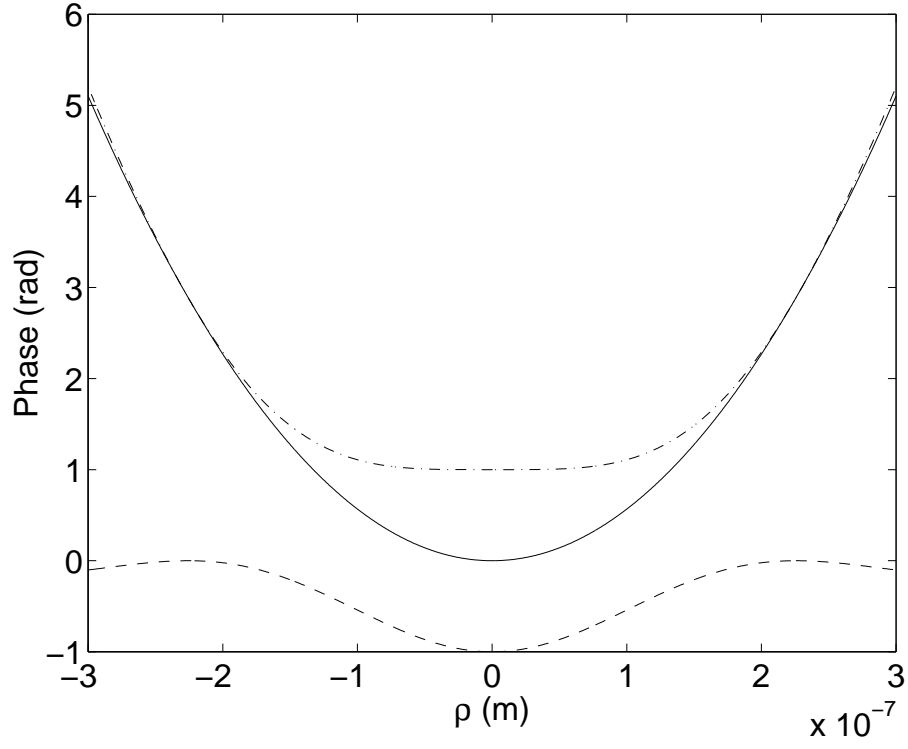


FIG. 6: The wavefront aberrations when $A=-1$. The solid line shows $\pi\rho^2/\lambda_D f$, the dashed line $-AJ_0^2(k\rho)$ and the dash-dotted line $\Phi(\rho)$. Note that only in a small area around the optical focal point the phase function is constant (which means that the aberrations are small).

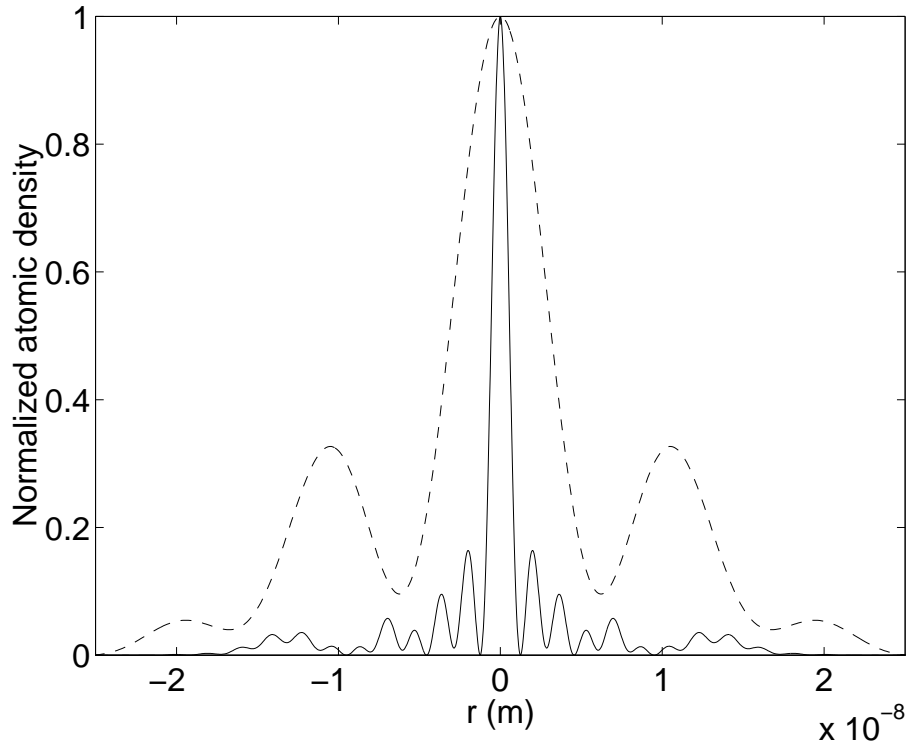


FIG. 7: The atomic density when $A=-100$ (solid line) and $A=-20$ (dashed line).

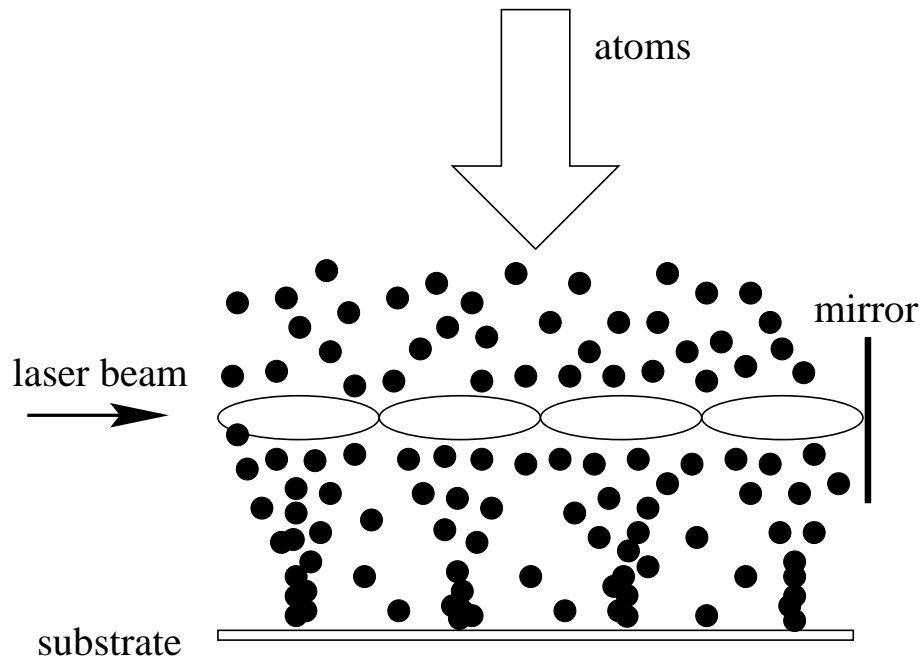


FIG. 8: Deposition of atoms on a substrate using a standing wave.

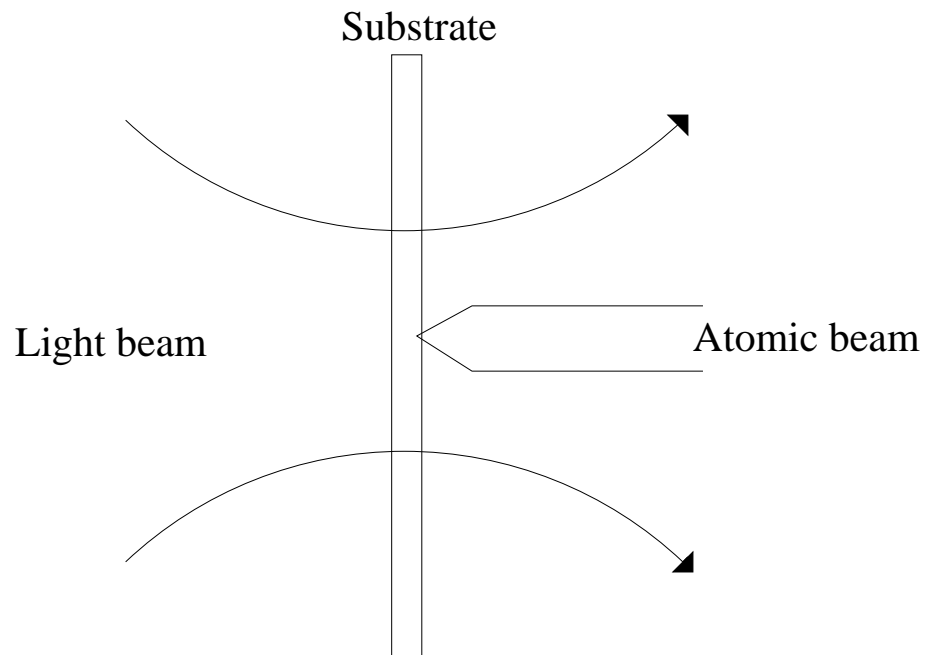


FIG. 9: Deposition of atoms on a transparent substrate with a focused light beam.